The Journal of Toxicological Sciences (J. Toxicol. Sci.)
Vol.39, No.4, 551-559, 2014

Original Article

Comparing the role of silica particle size with mineral fiber geometry in the release of superoxide from rat alveolar macrophages

Masayuki Ohyama[1], Hideki Tachi[2], Chika Minejima[3] and Takayuki Kameda[4]

[1]Department of Environmental Health, Osaka Prefectural Institute of Public Health, 1-3-69, Nakamichi, Higashinari-ku, Osaka 537-0025, Japan
[2]Department of Textile & Polymer Section, Technology Research Institute of Osaka Prefecture, 2-7-1, Ayumino, Izumi Osaka 594-1157, Japan
[3]Department of Material Science, College of Liberal Arts, International Christian University, 3-10-2, Osawa, Mitaka Tokyo 181-8585, Japan
[4]Graduate School of Energy Science, Kyoto University, Yoshida-Honmachi, Sakyo-ku, Kyoto 606-8501, Japan

(Received March 25, 2014; Accepted May 19, 2014)

ABSTRACT — Particulate air pollutants and mineral fibers activate inflammatory cells to release oxidants, which contribute to inflammation and injury in the lower respiratory tract. Our aim was to compare the role of silica particle size with mineral fiber length and width in the ability to induce superoxide release from rat alveolar macrophages. We estimated the ability of four types of silica particle samples, with different mode diameter, and three types of mineral fiber samples, with different geometric mean lengths and widths, to induce lucigenin-dependent chemiluminescence (CL) from the cells per number of dust particles (i.e., silica particles and mineral fibers). A close positive correlation was observed between dust size and the ability to induce CL in silica as well as mineral fiber samples. Moreover, the ability of silica samples to induce CL was weaker than that of long mineral fiber sample. This ability increased at a larger rate in small silica particle and thin mineral fiber samples than in large silica particle and thick mineral fiber samples at the initial stage of administration. These results suggest that the kinetics of the induction superoxide release from macrophages is similar between silica particles and mineral fibers; moreover, this depends on silica particle size and mineral fiber geometry. Finally, large silica particles were more active than small ones.

Key words: Silica, Quartz, Man-made mineral fibers, Reactive oxygen species, Superoxide, Macrophage

INTRODUCTION

Particulate air pollutants [including ultrafine particles (UFPs), particulate matter (PM) under 2.5 μm in diameter (PM2.5), PM under 10 μm in diameter (PM10), diesel exhaust particles, and silica particles] and mineral fibers (including asbestos and man-made mineral fibers) activate inflammatory cells to release oxidants such as superoxide anion, hydrogen peroxide, and hydroxyl radicals (Ciencewicki *et al.*, 2008). Oxidants can contribute to inflammation and injury in the lower respiratory tract, and oxidants from macrophages may play a central role in the biological effects of various dusts (Rom, 2011). The biological effects of these particles have been studied. For example, chronic exposure to UFPs produces deleterious effects on the lung; UFPs also cause oxidative stress and enhance proinflammatory effects in airways of patients with chronic obstructive pulmonary disease (Mehta *et al.*, 2008). Moreover, occupational exposure to crystalline silica is associated with the development of pulmonary silicosis (Reiser and Last, 1979), and alveolar macrophages play a critical role in the biological effects of silica particles (Davis, 1986). However, no clear relationship exists between particle size and the ability to induce oxidant release from macrophages. We previously suggested that macrophages non-specifically induce the release of superoxide on exposure to different types of mineral fibers, depending on fiber length; moreover, the increase rate of

Correspondence: Masayuki Ohyama (E-mail: ohyama@iph.pref.osaka.jp)

the ability to induce chemiluminescence (CL) depends on fiber width. We demonstrated a strong correlation between geometric-mean fiber length and the ability to induce CL (largest $r^2 = 0.9760$) and a negative correlation between geometric-mean fiber width and the increase rate of the ability to induce CL (largest $r^2 = 0.7473$) in seven types of mineral fibers (Ohyama *et al.*, 2000, 2001). Therefore, we consider that the reactivity of the superoxide response from macrophages not only depends on fiber geometry but also on particle size.

Alveolar macrophages play a critical role in the process of fibrosis caused by silica particles and mineral fibers (Davis, 1986; Mossman and Churg, 1998). Zhang *et al.* (2000) reported that superoxide from macrophages mediates silica genotoxicity.

In contrast, in non-asbestos mineral fiber (i.e., man-made mineral fibers) studies, fiber length has been found to be a major descriptor of tumorigenicity (Stanton *et al.*, 1981; Roller *et al.*, 1996). Further, larger α-quartz crystals have been reported to produce severe inflammation and fibrosis in an instillation experiment (Wiessner *et al.*, 1989; Goldstein and Webster, 1966).

The purpose of this study was to compare the role of silica particle size with mineral fiber geometry in the ability to induce superoxide release from rat alveolar macrophages. Although PM includes many components, the role of only silica particle size was investigated in the present study.

MATERIALS AND METHODS

Mineral samples

Particles: Silica (S-5631, Particle size: 0.5-10 μm) was obtained from Sigma Chemical Co. (St. Louis, MO, USA). We suspended silica particles in distilled water, and four samples (A, B, C and D) of different particle sizes were obtained depending on the sedimentation rate of the suspension. The diameters of particles in the four samples were measured using a laser scattering particle size distribution analyzer (LA-700, Horiba Ltd., Kyoto, Japan). Silica particle numbers per unit weight were counted using a hemocytometer under an optical microscope (Microphot-FX, Nikon Co., Tokyo, Japan) (objective lens: (20; eyepiece: (10; intermediate magnifier: (2; resolving power of lens: $\lambda/2N.A. = 0.3667$ μm, where $\lambda = 0.55$ μm and numerical aperture (N.A.) = 0.75). We used an X-ray diffractometer (Rint-1100, Rigaku Co., Tokyo, Japan) for identification of silica samples. The form of silica in all silica samples was α-quartz.

Mineral fibers: We used the Japan Fibrous Material standard reference samples provided by the Japan Association for the Study of Fiber Materials (Tokyo, Japan). The fiber samples were rock wool (RW1, geometric-mean length: 16.5 μm; geometric-mean width: 1.8 μm; number of fibers per unit weight: 1.7×10^3/μg), refractory ceramic fiber (RF1, 12.0, 0.77, and 8.8, respectively), and silicon carbide whisker (SC1, 6.4, 0.30, and 410, respectively). The characterization of these fibers has been documented elsewhere (Kohyama *et al.*, 1997; Yamato *et al.*, 1998). For example, chemical composition of these fibers has been demonstrated by X-ray fluorescence analysis. Silicon was the common and principal element in these fiber samples (RW1, chemical composition of SiO_2: 36%, Al_2O_3: 13%, CaO: 43%; RF1, SiO_2: 50%, Al_2O_3: 49%; SC1, SiC: 99.6%). Fe_2O_3 was the only iron compound detected in these samples (RW1, chemical composition of Fe_2O_3: 0.41%; RF1, 0.15%; SC1, 0.07%).

All particle and fiber samples were dried and heat-sterilized at 80°C for 48 hr and suspended in fetal bovine serum (FBS) at concentrations of 1 mg/ml. The suspensions were incubated for 15 min at 37°C, and spin-washed three times in Hanks' balanced salt solution (HBSS) at $900 \times g$ for 20 min. Pellets were resuspended at 0.77, 3.08, and 5.38 mg/ml, except SC1, which was adjusted to one-tenth the concentration of other samples. These suspensions were stored at 4°C.

Cell isolation

The experiments were conducted on 6 week-old male F344 rats obtained from Japan SLC, Inc. (Hamamatsu, Japan) that were placed in a clean air exposure chamber at room temperature of 25 ± 2°C 1-2 week with food and water *ad libitum*. The exposure chamber system has been described (Ohyama *et al.*, 2010). In brief, clean air was supplied by filtering room air with approximately 5 kg of activated granular charcoal and 15 sheets of American air filter for vinyl isolator (Clea Japan, Inc., Tokyo, Japan). The wind velocity in the chambers was suppressed to less than 0.05 m/sec.

Bronchoalveolar lavage was performed on the domesticated F344 rats to isolate alveolar macrophages for *in vitro* experiments. Briefly, rats were injected peritoneally with 5% pentobarbital sodium at 25 mg/kg. The lungs were lavaged with cold (4°C) HBSS containing 100 U of penicillin and 100 μg of streptomycin per 1 ml with a 10 ml plastic syringe. This process was repeated until a total of 50 ml lavage fluid was collected. The lavage fluid was centrifuged at 250 × g, for 10 min at 4°C. The pellet was resuspended in 5 ml of RPMI-1640 medium (HEPES modification, Sigma Chemical Co.) with 10% FBS and penicillin (100 U/ml) and streptomycin (100 μg/ml). A smear of Giemsa Stain Solution (Wako

Pure Chemical Industries, Ltd., Osaka, Japan) and part of the cell suspension was used to confirm that granulocyte content was less than 5%. In all experiments, the viability of cells was higher than 95% as measured by the trypan blue exclusion test. The suspension stored at 4°C until an assay. All procedures associated with this study were reviewed and approved by the Institutional Animal Care and Use Committee at Osaka Prefectural Institute of Public Health.

CL measurements

The method for measuring lucigenin-dependent CL from the macrophages exposed to various sample dust particles has been described in previous reports (Ohyama *et al.*, 2001; Nyberg and Klockars, 1990; Ohyama *et al.*, 2000).

The isolated cells (1.5×10^5) were transferred to a luminometer tube containing sample suspension (65 µl), 10% FBS, 0.1 mM lucigenin, and in some experiments 1,000 unit/ml superoxide dismutase (SOD). The final volume of each tube was 1 ml. The light emission of each sample was detected at 15-min intervals using a luminescence reader (ALOKA BLR-201, Mitaka, Tokyo, Japan). The CL response of all samples, including the negative control (no dust), was measured at constant rotation every 15 min using a stock suspension of cells. We performed all reactions at 37°C in RPMI 1640, and each measurement three times.

Statistical analysis

We estimated the ability to induce CL per sample fiber for exclusion of sample dose effects, as described previously (Ohyama *et al.*, 2000, 2001). Briefly, we plotted the relationships between the administered numbers of fiber samples and CL response by each of the samples. A slope (β_1) of linear regression of the administered numbers of fiber samples and CL was estimated as the ability to induce CL per sample fiber. As β_1 was a constant, it was possible to universally compare with each sample and to examine relationship between the ability to induce CL and fiber geometries. For example, we examined the relationship between geometric-mean length of fibers and β_1 by linear regression; we found a strong correlation between them (largest $r^2 = 0.9760$). Moreover, we calculated the increase rate with two continuous β_1 over a time course, and examined the relationship between fiber width and the increase rate of β_1; we found a negative correlation between them (largest $r^2 = 0.7473$). The accuracy of this analysis is dependent on the linearity of the relationship between the fiber dose (number) and CL response. Therefore, it is important to experiment within the high linearity between dose and response in each sample. The dose was reduced for SC1.

RESULTS

Silica size and dust number per unit weight

Table 1 shows the results of silica samples from the laser scattering particle size distribution analyzer, and the results of particle number per unit weight of silica samples using a hemocytometer and an optical microscope. Each diameter at 90% distribution was considerably different. However, according to the laser scattering particle size distribution analysis, the proportion of particles under 0.51 µm was similar in four samples. We used the mode diameter (maximal value of distribution) as the particle size.

The silica particle numbers in Table 1 represent the number confirmed using an optical microscope. As the proportion of particles under 0.51 µm was similar in the four samples, it was assumed that the ratios of silica particle numbers shown in Table 1 were approximate with those of silica particle numbers including unconfirmed particles using the microscope.

Relationship between CL and sample weight

We measured the CL response of all samples at constant rotation every 15 min using the same stock suspension of cells. The CL response of each sample increased

Table 1. Particle diameter and number per unit weight of silica samples

Sample	A	B	C	D
median diameter (µm)	3.79	2.89	0.99	0.68
mode diameter (µm)	6.72	5.87	2.27	1.15
diameter %: 10.00 µm (%)	97.3	99.2	100	100
diameter %: 0.51 µm (%)	34.1	33.5	33.5	36.7
% diameter: 90.0% (µm)	8.09	6.71	2.95	1.39
number per unit weight (/µg)	6,650	9,255	55,286	340,500

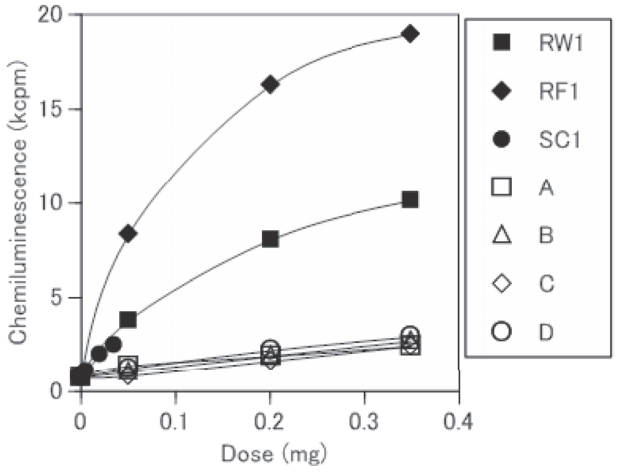

Fig. 1. The relationship between sample weight and CL response at 45 min.

in a time-dependent manner, and the relative relationship of the samples was similar at each time point. However, the CL response in many samples decreased after 90 min. Fig. 1 shows a representative relationship between sample weight and CL at 45 min, because the time-dependent CL response of all samples gradually increased at 30-75 min. Although four silica samples had particles with different diameters and numbers per unit weight, in comparison with the sample dose, they induced similar levels of CL. However, the orders of CL values in the samples fluctuated each time. No role was observed in the order results upon comparison with the sample dose. In comparison with the sample dose, three mineral fiber samples induced higher levels of CL than four silica particle samples.

Time course of the ability to induce CL per dust particle (β_1)

We calculated β_1 to compare the CL response of each sample at a value not related to the number of dust particles administered. Table 2 shows β_1 and r^2 values of the regression line with CL and number of dust particles. All samples dose-dependently induced a CL response. Each response was almost completely inhibited by SOD, which is a superoxide scavenger (data not shown). Although the relative relation of β_1 was similar at each time point, samples with large silica particles tended to gradually enhance β_1 at 15-75 min. Fig. 2 shows a representative relationship between the number of dust particles and CL at 45 min, because the β_1 of all samples gradually increased at 30-75 min. The ability to induce CL tended to depend on the diameter of the particles and length of the fibers. Long mineral fibers (RW1 and RF1) were more active than the four silica particle samples. Similar length fibers (SC1) with the mode diameter of silica (A and B) particles were less active than silica particles in samples A and B.

Relationship between dust size and β_1

Fig. 3 shows a representative relationship between dust size (mode diameter of particles and geometric-mean length of fibers) and β_1 in the two groups (silica particles and mineral fibers) at 45 min. A close correlation was found between dust particle size and β_1 in both the groups at 15-120 min. However, the intersection of the regression line of the silica samples and mineral fiber samples with the horizontal axis was 1.27 ± 0.11 and 6.96 ± 0.11 μm (average ± standard deviation) at 15-120 min, respectively. Table 3 presents the slope (i.e., β_2) and r^2 of the regres-

Table 2. Slope (β_1) and r^2 of the regression lines for CL and number of dust particles

Time[a]	0		15		30		45		60		75		90		105		120	
	β_1[b]	r^2[c]	β_1	r^2	β_1	r^2	β_1	r^2	β_1	r^2	β_1	r^2	β_1	r^2	β_1	r^2	β_1	r^2
A	-0.62	0.59	25.24	0.73	40.47	0.99	66.19	0.95	103.9	0.97	151.3	0.99	174.7	0.98	166.4	0.95	145.6	0.95
B	-0.07	0.01	18.80	0.72	35.44	1.00	59.92	1.00	101.5	1.00	139.2	0.99	148.4	0.99	139.5	0.96	118.6	0.95
C	-0.03	0.05	1.16	0.54	4.11	0.96	8.97	0.99	15.51	0.99	22.87	0.99	25.38	0.99	23.36	0.96	19.01	0.92
D	-0.01	0.86	0.11	0.14	1.19	0.99	1.80	0.99	2.48	1.00	3.19	0.99	3.74	0.99	3.76	0.97	3.46	0.96
RW1	1.49	0.06	501.6	0.98	1103	0.96	1,517	0.94	1,708	0.94	1,722	0.95	1,656	0.96	1,529	0.96	1,374	0.97
RF1	-0.35	0.66	241.4	0.96	454.4	0.92	553.8	0.88	603.5	0.85	603.6	0.84	553.2	0.83	491.9	0.82	415.8	0.81
SC1	-0.04	0.32	0.86	0.60	6.12	1.00	12.1	0.98	15.5	1.00	19.41	1.00	22.2	0.99	22.48	1.00	23.00	0.99

[a]Time after administration (min). [b]β_1 ($\times 10^{-8}$) is the slope of the regression line for the estimated number of dust particles administered and CL response with three concentrations and a duplicate negative control. The CL response is the mean value of the three measurements. [c]Square of the correlation coefficient of the regression line.

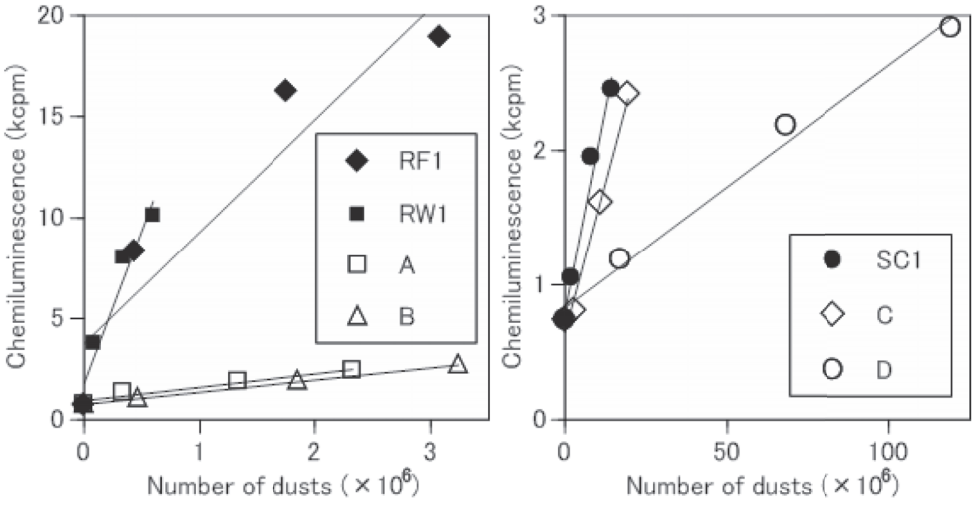

Fig. 2. The relationship between number of dust particles and CL response at 45 min. The lines represent regression lines (RF1: $y = 553.8 \times 10^{-8}x + 374.6 \times 10^{-8}$; RW1: $y = 1517 \times 10^{-8}x + 178.4 \times 10^{-8}$; A: $y = 66.2 \times 10^{-8}x + 92.3 \times 10^{-8}$; B: $y = 59.9 \times 10^{-8}x + 74.3 \times 10^{-8}$; SC1: $y = 12.1 \times 10^{-8}x + 80.0 \times 10^{-8}$; C: $y = 9.0 \times 10^{-8}x + 64.4 \times 10^{-8}$; and D: $y = 1.8 \times 10^{-8}x + 82.6 \times 10^{-8}$). The slope ($\beta_1$) of the line was taken as a measure of the ability to induce CL per dust particle.

Table 3. Slope (β_2) and r^2 of the regression lines for β_1 in Table 2 and dust size

Time[a]	15		30		45		60		75		90		105		120	
	β_2[b]	r^2[c]	β_2	r^2	β_2	r^2	β_2	r^2	β_2	r^2	β_2	r^2	β_2	r^2	β_2	r^2
Silica[d]	4.606	0.98	7.524	0.99	12.32	0.99	19.9	0.98	28.28	0.99	31.8	1.00	30.06	1.00	26.1	0.99
Fiber[e]	49.31	0.99	107.5	0.97	146.9	0.95	165.1	0.95	166	0.94	159.1	0.93	146.5	0.93	131.2	0.91
Ratio[f]	10.71		14.29		11.92		8.30		5.87		5.00		4.87		5.03	

[a]Time after administration (min). [b]β_2 ($\times 10^{-8}$) is the slope of the regression line for β_1 in Table 2 and dust size (mode diameter of silica samples or geometric-mean length of fibers). [c]Square of the correlation coefficient of the regression line for β_1 in Table 2 and dust size. [d]Group of four silica samples. [e]Group of three mineral fiber samples. [f]β_2 of fiber / β_2 of silica

sion lines with dust size and β_1. A close correlation was found between dust particle size and β_1 at each time-point in both the groups. Long mineral fibers were more active than large silica particles. β_2 of mineral fiber samples was 8.25 ± 3.66 times higher than that of silica samples at the average measurement period using mode diameter. However, silica particles in samples A and B were more active than similar length sized fibers (SC1).

Role in the increase rate of β_1

We calculated the increase rate of β_1 to compare the response pattern to each sample (Fig. 4). In the power regression, there was a close correlation between time and the increase rate of β_1 in mineral fiber samples; however, silica particle samples showed various response patterns. The response patterns of silica particles in samples B and C were similar to those of mineral fiber samples. Moreover, the reason for the various response patterns of silica particles in samples A and D were that the particles in samples A and D showed a low and high value of the increase rate of β_1 at 15-30 min, respectively. Both smaller particles and thinner fibers cause a larger acceleration in increase rate of β_1 at the initial phase. The relationship between dust size and increase rate of β_1 at 15-30 min is shown in Fig. 5. Silica particle samples had a close correlation between mode diameter and the increase rate of β_1 in the power regression only at 15-30 min ($r^2 = 0.9544$). The time-dependent decrease of the increase rate of β_1 was rapid for silica particles in sample D and slow for those in sample A. Mineral fiber samples showed a correlation between fiber width and the increase rate of β_1 ($r^2 = 0.6808$). The order of values of the increase rate

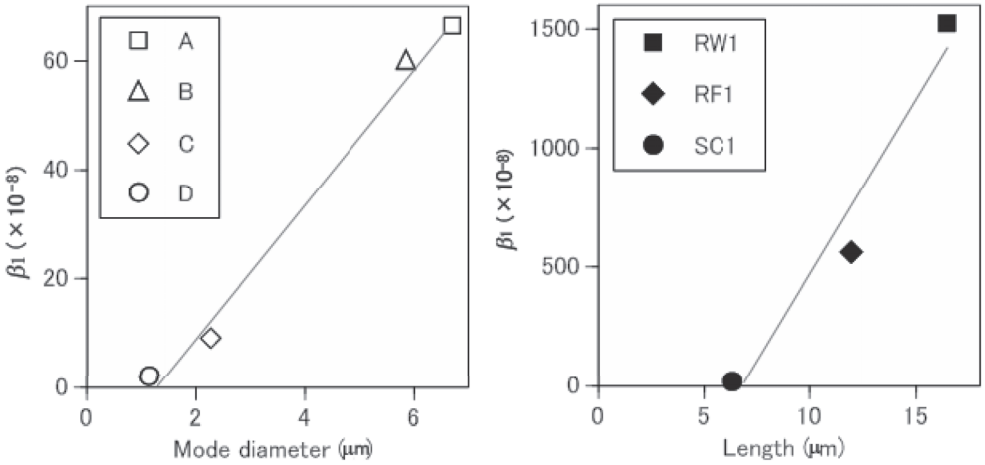

Fig. 3. The relationship between dust size (mode diameter of particles and geometric-mean length of fibers) and β_1 in Table 2. The lines represent regression lines (Silica: y = 12.32 × 10^{-8}x – 15.08 × 10^{-8}; Fiber: y = 146.9 × 10^{-8}x + 1015 × 10^{-8}). Data at 45 min.

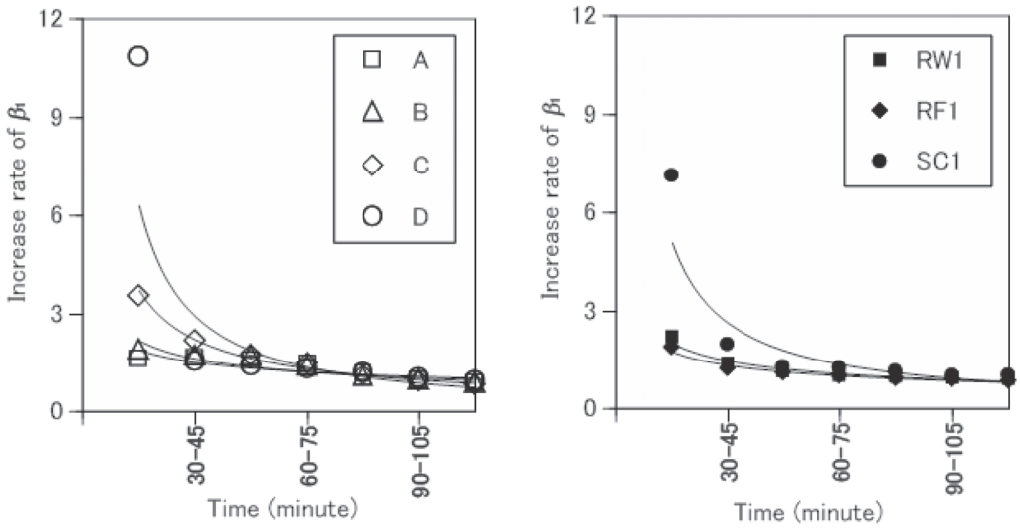

Fig. 4. Time course of increase rate of β_1. The lines represent power regression lines. A: r^2 = 0.685; B: r^2 = 0.826; C: r^2 = 0.985; D: r^2 = 0.791; RW1: r^2 = 0.951; RF1: r^2 = 0.961; and SC1: r^2 = 0.868 (r^2 is square of the correlation coefficient of power regression).

of β_1 did not fluctuate with time in mineral fiber samples. Although both smaller particles and thinner fibers caused larger acceleration and increased the rate of β_1 at the initial phase, the silica relationship did not continue.

DISCUSSION

We found a close positive correlation between the size of silica particles and the ability to induce CL from rat alveolar macrophages per number of silica particles. Furthermore, the ability of silica samples to induce CL was weaker than that of long fiber samples; this ability induced at a larger rate in small particle and thin fiber samples than large particle and thick fiber samples at the initial stage of administration. However, silica particles were more active than mineral fibers (dust size under 7 μm) and silica particles that were approximately less than 1 μm were less active.

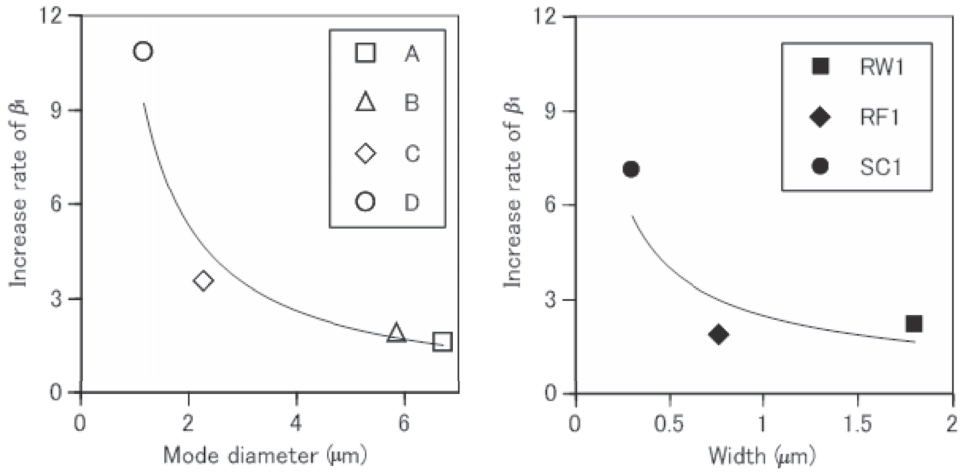

Fig. 5. The relationship between dust particle size (mode diameter of particles and geometric-mean width of fibers) and increase rate of β_1. Silica: $r^2 = 0.954$; and Fiber: $r^2 = 0.681$ (r^2 is square of the correlation coefficient of power regression). Data at 15-30 min.

These results suggest that depending on dust size, the kinetics of the induction of superoxide release from macrophages is similar between silica particles and mineral fibers. On considering per sample weight, there were no clear differences in the CL responses between the four silica samples. However, on considering per dust particle number, large silica particles were more active than small ones; the ability of large silica particles to induce CL was slowly enhanced in comparison with that of small ones. Further, the role of mode diameter of silica particles coincided with the role of length and width of mineral fibers.

Epidemiological and pathological studies have established that occupational exposure to crystalline silica is associated with the development of pulmonary silicosis (Reiser and Last, 1979) and an increased risk for lung cancer (IARC, 1997). However, only experiments using rats have demonstrated the carcinogenicity of silica (Wagner *et al.*, 1980; Hessel *et al.*, 2000). The pulmonary response to silica considerably varies across different species, with mice developing silicosis but no lung cancer and hamsters simply showing the storage of silica in lung macrophages with no apparent pathology (IARC, 1987; Saffiotti, 1992).

A similar phenomenon is reported with non-asbestos mineral fibers. For example, on exposure to certain mineral fibers, hamsters do not develop lung tumors, whereas rats show a relatively high incidence of lung tumors (Mast *et al.*, 1994; Hesterberg *et al.*, 1995).

Our findings are consistent with the finding that alveolar macrophages play an important role in the process of fibrosis caused by silica particles and mineral fibers. Moreover, our results suggest that long fibers contribute to a greater extent to lung injury than silica particles. It is notable that Dörger *et al.* (2000) reported that in comparison with hamster alveolar macrophages, rat alveolar macrophages release higher amounts of superoxide, supporting the important role of reactive oxygen species (ROS) in fiber-induced lung disorders, as the incidence of lung tumors was higher in rats than in hamsters.

The phenomenon of rat lung overload following exposure to low-toxicity particles has recently received considerable attention because of its importance in extrapolating data for human risk assessment (ILSI, 2000). Several toxicological studies have documented increased toxicity of materials in the form of UFPs compared to the same mass of materials in the form of FPs (Donaldson and Tran, 2002). A clue to the mechanism underlying this difference may be found in the fact that a given mass of UFPs has a much greater surface area than the same mass of FPs.

However, our results suggest that particles under 1 μm (including UFPs) are not efficient at inducing superoxide release in large quantities from macrophages. Moreover, we previously showed that a sample of PM induces much more superoxide from macrophages than a sample of silica with similar particle size (Ohyama *et al.*, 2007) and that the superoxide response by macrophages to PM is similar to that of 3-nitrobenzanthrone-coated non-reactive particles (Ohyama *et al.*, 2012). Therefore, the superoxide response by macrophages is not dependent on particle size only. We believe that it is necessary to notice particle aggregation in overload experiments caused by low-toxicity particles and that it is necessary to consider the effects

of some components in ultrafine air pollutants.

Both *in vitro* and *in vivo* experiments indicate a causal relationship between ROS and development of silica-induced cell damage, inflammation, and pulmonary fibrosis (Dörger *et al.*, 2000; Huang *et al.*, 1998; Castranova, 1994; Janssen *et al.*, 1994; Yamano *et al.*, 1995). However, silica is not directly genotoxic (Sobti and Bhardwaj, 1991; Driscoll *et al.*, 1997), and Janssen *et al.* (1992) indicated that exposure to silica causes a dramatic increase in the steady-state levels of manganese-containing SOD mRNA and that exposure to asbestos results in an overall increase in catalase activity. Moreover, Zhang *et al.* (2000) observed that superoxide from macrophages mediates silica genotoxicity. These results suggest that the amount of superoxide released from macrophages reflects the genotoxicity or biological effects of various mineral dust particles. Therefore, our results are consistent with other *in vivo* tumorigenicity studies on mineral dust particles.

In conclusion, our results indicate that alveolar macrophages play a critical role in the biological effects of silica particles and non-asbestos mineral fibers. Our results suggest that the kinetics of the induction of superoxide release from macrophages is similar between silica particles and mineral fibers; moreover, particles that are under 1 μm are not efficient at inducing superoxide release in large quantities from macrophages.

ACKNOWLEDGMENTS

The authors thank the Japan Association for the Study of Fiber Materials for supplying the Japan Fibrous Material standard reference samples. This study was supported by a Grant-in-Aid for Scientific Research from the Ministry of Education, Culture, Sports, Science and Technology.

REFERENCES

Castranova, V. (1994): Generation of oxygen radicals and mechanisms of injury prevention. Environ. Health Perspect., **102 (Suppl)**, 65-68.

Ciencewicki, J., Trivedi, S. and Kleeberger, S.R. (2008): Oxidants and the pathogenesis of lung diseases. J. Allergy Clin. Immunol., **122**, 456-468.

Davis, G.S. (1986): Pathogenesis of silicosis: current concepts and hypotheses. Lung, **164**, 139-154.

Donaldson, K. and Tran, C.L. (2002): Inflammation caused by particles and fibers. Inhal. Toxicol., **14**, 5-27.

Dörger, M., Munzing, S., Allmeling, A.M. and Krombach, F. (2000): Comparison of the phagocytic response of rat and hamster alveolar macrophages to man-made vitreous fibers *in vitro*. Hum. Exp. Toxicol., **19**, 635-640.

Driscoll, K.E., Deyo, L.C., Carter, J.M., Howard, B.W., Hassenbein, D.G. and Bertram, T.A. (1997): Effects of particle exposure and particle-elicited inflammatory cells on mutation in rat alveolar epithelial cells. Carcinogenesis, **18**, 423-430.

Goldstein, B. and Webster, I. (1966): Intratracheal Injection into rats of size-graded silica particles. Brit. J. Ind. Med., **23**, 71-74.

Hessel, P.A., Gamble, J.F., Gee, J.B., Gibbs, G., Green, F.H., Morgan, W.K. and Mossman, B.T. (2000): Silica, silicosis, and lung cancer: a response to a recent working group report. J. Occup. Environ. Med., **42**, 704-720.

Hesterberg, T.W., Miiller, W.C., Thevenaz, P. and Anderson, R. (1995): Chronic inhalation studies of man-made vitreous fibres: characterization of fibres in the exposure aerosol and lungs. Ann. Occup. Hyg., **39**, 637-653.

Huang, S.H., Leonard, S., Shi, X., Goins, M.R. and Vallyathan, V. (1998): Antioxidant activity of lazaroid (U-75412E) and its protective effects against crystalline silica-induced cytotoxicity. Free Radic. Biol. Med., **24**, 529-536.

IARC (1987): Silica and Some Silicates. IARC Monogr. Eval. Carcing. Risks Chem. Hum., **42**, 1-239.

IARC (1997): Silica, some silicates, coal dust and para-aramid fibrils. IARC Monogr. Eval. Carcing. Risks Hum., **68**, 41-244.

ILSI Risk Science Institute (2000): The relevance of the rat lung response to particle overload for human risk assessment: A workshop consensus report. Inhal. Toxicol., **12**, 1-17.

Janssen, Y.M., Marsh, J.P., Absher, M.P., Hemenway, D., Vacek, P.M., Leslie, K.O., Borm, P.J. and Mossman, B.T. (1992): Expression of antioxidant enzymes in rat lungs after inhalation of asbestos or silica. J. Biol. Chem., **267**, 10625-10630.

Janssen, Y.M., Marsh, J.P., Driscoll, K.E., Borm, P.J., Oberdörster, G. and Mossman, B.T. (1994): Increased expression of manganese-containing superoxide dismutase in rat lungs after inhalation of inflammatory and fibrogenic minerals. Free Radic. Biol. Med., **16**, 315-322.

Kohyama, N., Tanaka, I., Tomita, M., Kudo, M. and Shinohara, Y. (1997): Preparation and characteristics of standard reference samples of fibrous minerals for biological experiments. Ind. Health, **35**, 415-432.

Mast, R.W., Hesterberg, T.W., Glass, L.R., McConnell, E.E., Anderson, R. and Bernstein, D.M. (1994): Chronic inhalation and biopersistence of refractory ceramic fiber in rats and hamsters. Environ. Health Perspect., **102 (Suppl)**, 207-209.

Mehta, M., Chen, L.C., Gordon, T., Rom, W. and Tang, M.S. (2008): Particulate matter inhibits DNA repair and enhances mutagenesis. Mutat. Res., **657**, 116-121.

Mossman, B.T. and Churg, A. (1998): Mechanisms in the pathogenesis of asbestosis and silicosis. Am. J. Respir. Crit. Care Med., **157**, 1666-1680.

Nyberg, P. and Klockars, M. (1990): Measurement of reactive oxygen metabolites produced by human monocyte-derived macrophages exposed to mineral dusts. Int. J. Exp. Path., **71**, 537-544.

Ohyama, M., Otake, T. and Morinaga, K. (2000): The chemiluminescent response from human monocyte-derived macrophages exposed to various mineral fibers of different sizes. Ind. Health, **38**, 289-293.

Ohyama, M., Otake, T. and Morinaga, K. (2001): Effect of size of man-made and natural mineral fibers on chemiluminescent response in human monocyte-derived macrophages. Environ. Health Perspect., **109**, 1033-1038.

Ohyama, M., Otake, T., Adachi, S., Kobayashi, T. and Morinaga, K. (2007): A comparison of the production of reactive oxygen species by suspended particulate matter and diesel exhaust particles

with macrophages. Inhal. Toxicol., **19 (Suppl)**, 157-160.

Ohyama, M., Oka, K., Adachi, S. and Takenaka, N. (2010): Effects of nitrous acid exposure on pulmonary tissues in guinea pigs. Inhal. Toxicol., **22**, 930-936.

Ohyama, M. Akasaka, S., Otake, T, Morinaga, K., Kim, Y.W., Moon, K.W., Kameda, T. and Adachi, S. (2012): Effects of atmospheric particles and several model particles of particulate matter components on human monocyte-derived macrophage oxidative responses. J. Clinic. Toxicol., **2**, doi.org/10.4172/2161-0495.1000121.

Reiser, K.M. and Last, J.A. (1979): Silicosis and fibrogenesis: fact and artifact. Toxicology, **13**, 51-72.

Rom, W.N. (2011): Role of oxidants in interstitial lung diseases: pneumoconioses, constrictive bronchiolitis, and chronic tropical pulmonary eosinophilia. Mediators Inflamm., doi: 10.1155/2011/407657.

Roller, M., Pott, F., Kamino, K., Althoff, G.H. and Bellmann, B. (1996): Results of current intraperitoneal carcinogenicity studies with mineral and vitreous fibres. Exp. Toxicol. Pathol., **48**, 3-12.

Saffiotti, U. (1992): Lung cancer induction by crystalline silica. Prog. Clin. Biol. Res., **374**, 51-69.

Sobti, R.C. and Bhardwaj, D.K. (1991): Cytogenetic damage and occupational exposure. I. Exposure to stone dust. Environ. Res., **56**, 25-30.

Stanton, M.F., Layard, M., Tegeris, A., Miller, E., May, M., Morgan, E. and Smith, A. (1981): Relation of particle dimension to carcinogenicity in amphibole asbestoses and other fibrous minerals. J. Natl. Cancer Inst., **67**, 965-975.

Wagner, M.M., Wagner, J.C., Davies, R. and Griffiths, D.M. (1980): Silica-induced malignant histiocytic lymphoma: incidence linked with strain of rat and type of silica. Br. J. Cancer, **41**, 908-917.

Wiessner, J.H., Mandel, N.S., Sohnle, P.G. and Mandel, G.S. (1989): Effect of particle size on quartz-induced hemolysis and on lung inflammation and fibrosis. Exp. Lung Res., **15**, 801-812.

Yamano, Y., Kagawa, J., Hanaoka, T., Takahashi, T., Kasai, H., Tsugane, S. and Watanabe, S. (1995): Oxidative DNA damage induced by silica *in vivo*. Environ. Res., **69**, 102-107.

Yamato, H., Morimoto, Y., Tsuda, T., Ohgami, A., Kohyama, N. and Tanaka, I. (1998): Fiber numbers per unit weight of JFM standard reference samples determined with a scanning electron microscope. Ind. Health, **36**, 384-387.

Zhang, Z., Shen, H.M., Zhang, Q.F. and Ong, C.N. (2000): Involvement of oxidative stress in crystalline silica-induced cytotoxicity and genotoxicity in rat alveolar macrophages. Environ. Res., **82**, 245-252.